

# The effect of creep exposure on microstructure stability and tensile properties of single crystal nickel based superalloy CMSX-4

J. Lapin\*, T. Pelachová, M. Gebura

*Institute of Materials and Machine Mechanics, Slovak Academy of Sciences,  
Račianska 75, 831 02 Bratislava, Slovak Republic*

Received 11 September 2012, received in revised form 16 November 2012, accepted 19 November 2012

## Abstract

The effect of creep exposure on microstructure stability and tensile properties of single crystal nickel-based superalloy CMSX-4 was studied. The single crystal samples with [001] crystallographic orientation were prepared by directional solidification in a Bridgman type of furnace. The creep exposure at 950 °C, applied stresses ranging from 60 to 230 MPa for various time up to 2000 h leads to the degradation of initial cuboidal  $\gamma/\gamma'$  microstructure. Coarsening of cuboidal  $\gamma'$  ( $\text{Ni}_3(\text{Al}, \text{Ti})$ ) precipitates, formation of transient microstructure consisting of coarsened  $\gamma'$  precipitates and rafts and finally development of well rafted  $\gamma/\gamma'$  microstructure are observed in the crept specimens. The width of the  $\gamma'$  rafts decreases and their length increases with increasing applied stress and creep time. The width of the  $\gamma$  (Ni-based solid solution) channels increases with increasing applied stress and creep time. The creep rafting decreases the offset yield stress and ultimate tensile strength in the temperature from range 20 to 950 °C when compared to those of the heat treated specimens with cuboidal  $\gamma/\gamma'$  microstructure. On the other hand, creep rafting increases significantly room and high temperature ductility of the studied alloy. The creep fracture surfaces exhibit palisade morphology formed by propagation of cracks along (001) crystallographic planes in directions perpendicular and parallel to loading direction.

**Key words:** nickel alloys, single crystal superalloy, creep, microstructure, mechanical properties

## 1. Introduction

Single crystal nickel based superalloy CMSX-4 is mainly used in aircraft engines and stationary gas turbines because of its ability to retain excellent combination of mechanical properties and corrosion resistance at high temperatures. The typical microstructure of this superalloy contains L1<sub>2</sub>-ordered  $\gamma'$  ( $\text{Ni}_3(\text{Al}, \text{Ti})$ ) precipitates (about 70 vol.%) coherently embedded in  $\gamma$  (Ni-based solid solution) matrix with face-centered cubic crystal structure [1–7]. During service the initial  $\gamma/\gamma'$  microstructure is subjected to degradation by the combined effect of temperature, mechanical stresses and environmental conditions. Three types of microstructure degradation affecting mechanical properties were observed: (i) growth of cuboidal  $\gamma'$  precipitates [2, 3]; (ii) spontaneous rafting formed preferentially within the dendrites during long-term ageing [6, 8,

9] and (iii) creep rafting [1, 2–4, 9–11]. The rafting process, i.e. directional coarsening of  $\gamma'$  precipitates might lead to a topological microstructure inversion such that the  $\gamma'$  phase becomes the matrix with rafts of the  $\gamma$  phase [12, 13]. While the rafting is not detrimental to creep rupture properties, it affects significantly tensile and fatigue properties [12, 13].

The aim of this article is to study the effect of creep exposure on microstructure stability and tensile properties of single crystal nickel based superalloy CMSX-4.

## 2. Experimental procedure

As-cast ingot of nickel base superalloy CMSX-4 with a diameter of 80 mm, length of 250 mm and chemical composition Ni-6.5Cr-9.0Co-0.6Mo-6.0W-6.5Ta-

\*Corresponding author: tel.: +421 2 49268290; fax: +421 2 49268312; e-mail address: [ummslapi@savba.sk](mailto:ummslapi@savba.sk)

-3.0Re-5.6Al-1.0Ti-0.1Hf (wt.%) was supplied by Canon-Muskegon (USA). The ingot was cut to smaller rectangular rods by electro-spark machining and lathe-machined to cylindrical rods with a diameter of 12 mm and length of 120 mm. Single crystals with [001] crystallographic orientation were prepared from single crystalline seeds by directional solidification at a temperature gradient in liquid at the solid-liquid interface of  $10^{\circ}\text{C mm}^{-1}$  and growth rate of  $100 \text{ mm h}^{-1}$  in a modified Bridgman type apparatus. Crystallographic orientation of directionally solidified bars was controlled by Laue X-ray diffraction technique. Maximum deviation from  $\langle 001 \rangle$  crystallographic direction was measured to be 7 degrees. The single crystal bars were subjected to solution annealing at  $1315^{\circ}\text{C}$  for 6 h in high purity argon atmosphere which was followed by a rapid cooling to room temperature in flowing argon. The heat treatment was finalized by two steps precipitation hardening at  $1140^{\circ}\text{C}$  for 2 h and  $870^{\circ}\text{C}$  for 20 h in air followed by gas fan cooling to room temperature.

Threaded head creep specimens were prepared by lathe machining from heat treated single crystal bars. The effect of creep exposure on stability of cuboidal  $\gamma/\gamma'$  type microstructure was studied at a temperature of  $950^{\circ}\text{C}$  using two types of cylindrical creep specimens. The specimens with multiple gauge sections with diameters of 3.1, 3.46, 4.0 and 4.9 mm and various gauge length ranging from 13.3 to 16.7 mm were subjected to creep testing at local applied stresses in the gauge sections of 60, 90, 120 and 150 MPa for various time up to 2000 h in air. The specimens with a gauge diameter of 6 mm and gauge length of 50 mm were subjected to creep testing at 230 MPa for 300 h in air. After creep, the specimens were machined to gauge diameter of 5 mm and used for tensile testing. Tensile tests were performed at six temperatures ranging from 20 to  $950^{\circ}\text{C}$  at an initial strain rate of  $1 \times 10^{-4} \text{ s}^{-1}$  using universal screw driven testing machine Zwick. The temperature of the specimens was controlled by K type thermocouple and tensile elongation was measured by high-temperature extensometer MAYTEC touching the gauge section.

Microstructural analysis was performed by optical microscopy (OM) and scanning electron microscopy (SEM). OM and SEM samples were prepared by grinding on abrasive papers, polished on diamond pastes up to a grain size of  $0.25 \mu\text{m}$  and etched in a reagent of 12.5 ml alcohol, 12.5 ml  $\text{HNO}_3$  and 13.5 ml HCl. Quantitative metallography was performed on digitalized micrographs using a computerized image analyser. Four basic microstructural parameters were evaluated on longitudinal sections of the creep specimens: (i) size of cuboidal  $\gamma'$  precipitates, (ii) width of  $\gamma'$  rafts, (iii) length of  $\gamma'$  rafts, and (iv) width of  $\gamma$  channels. All measured microstructural parameters

were evaluated statistically using appropriate distribution functions.

### 3. Results and discussion

#### 3.1. Microstructure after heat treatments

Figure 1 shows the typical microstructure of the creep specimens prepared from directionally solidified single crystal bars of CMSX-4 superalloy after the heat treatments. As shown by Gebura and Lapin [6, 8], the applied industrial type of heat treatments used in the present work decreases the degree of microsegregation in comparison with the microstructure after the directional solidification, as seen in Figs. 1a,b. However, certain degree of chemical heterogeneity between the dendrites and interdendritic region still remains and leads to small microstructural variations. This chemical heterogeneity cannot be fully eliminated even by solution annealing of the studied alloy at  $1315^{\circ}\text{C}$  for 120 h during which formation of recrystallized equiaxed grains was observed [9]. Figure 1c shows the typical  $\gamma/\gamma'$  microstructure of the heat treated CMSX-4 superalloy before creep testing. The quantitative metallographic analysis of the creep specimens shows that the cuboidal morphology is preserved and average volume fraction of the  $\gamma'$  precipitates (69.5 vol.%) is statistically the same within the dendrites and interdendritic region. All measured sizes of the  $\gamma'$  precipitates defined as their edge length are evaluated statistically using long-normal distribution function independently for the dendrites and interdendritic region (more than 3000 measurements for each region), as shown in Fig. 2. From this figure, it is clear that the mean size of the  $\gamma'$  precipitates of  $(281 \pm 2) \text{ nm}$  measured within the dendrites is lower than that of  $(316 \pm 2) \text{ nm}$  measured within the interdendritic region.

#### 3.2. Microstructure degradation during creep

Figure 3 shows geometry of creep specimen with multiple gauge sections and corresponding microstructures after creep testing at a temperature of  $950^{\circ}\text{C}$ , applied stresses of 60, 90, 120 and 150 MPa and creep time of 500 h. During the creep the cuboidal  $\gamma'$  precipitates within the interdendritic region undergo coarsening process at lower applied stresses and form a transient type of microstructure composed of cuboidal and rafted precipitates at higher applied stresses. The well-developed  $\gamma'$  rafts separated by the  $\gamma$  channels oriented nearly perpendicularly to the loading direction, which is parallel to the [001] crystallographic direction of the creep specimen, are developed within the dendrites. Three basic microstructural parameters were measured for the rafted microstructure: (i) width of the  $\gamma$  channels in a direction perpendicular

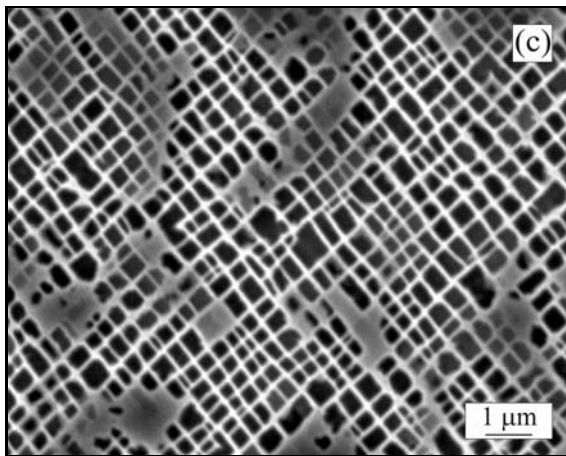
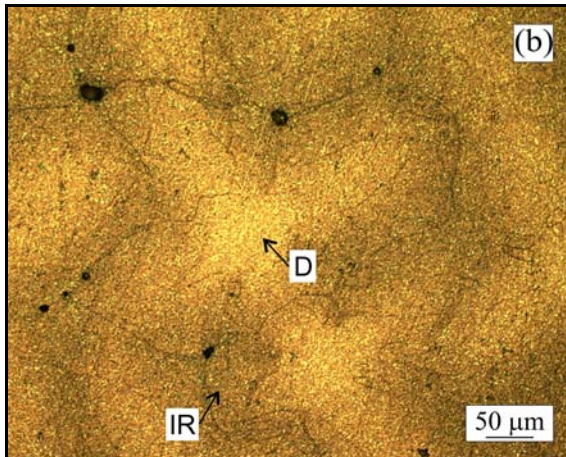
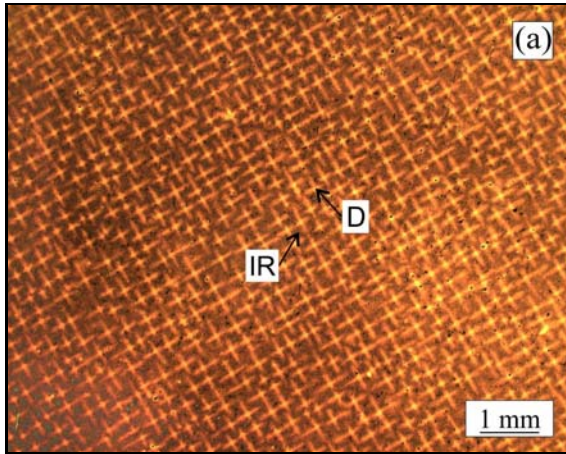


Fig. 1. The typical microstructure of single crystal CMSX-4 superalloy after heat treatments, D – dendrites, IR – interdendritic region: (a) dendritic microstructure on transversal section of the sample, OM; (b) chemical inhomogeneity between the dendrites and interdendritic region on transversal section of the sample, OM; (c) SEM micrograph showing cuboidal  $\gamma/\gamma'$  microstructure.

to the  $\gamma'$  rafts, (ii) width of the  $\gamma'$  rafts and (iii) length of the  $\gamma'$  rafts on longitudinal sections of the creep specimens. Figure 4 shows variation of the measured

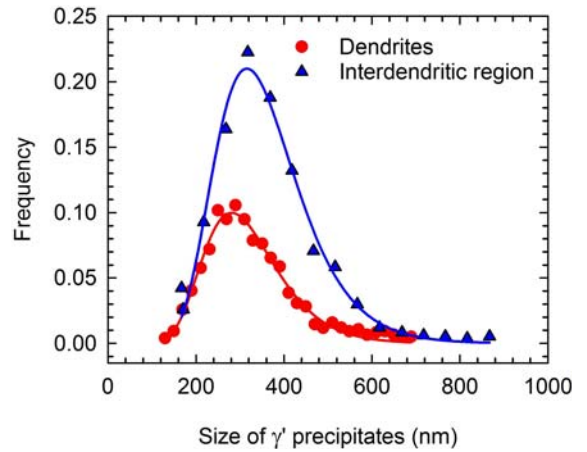


Fig. 2. Log-normal distribution curves of size of the  $\gamma'$  precipitates within the dendrites and interdendritic region.

microstructural parameters of the degraded  $\gamma/\gamma'$  microstructure with the applied stress after creep testing for various time. The values of the width of the  $\gamma'$  rafts in the specimens tested at 60 and 90 MPa for 100 h are affected by a transient type of microstructure between cuboidal and rafted one within the interdendritic region. For the degraded microstructure with well-developed rafts, the width of the  $\gamma'$  rafts decreases (Fig. 4a) and their length increases (Fig. 4b) with increasing applied stress and creep time. The width of the  $\gamma$  channels increases with increasing applied stress and creep time, as seen in Fig. 4c. As shown by Lapin et al. [5, 14], the cuboidal  $\gamma/\gamma'$  microstructure of the superalloy CMSX-4 is stable up to 2000 h at 950 °C and undergoes spontaneous rafting after 500 h at 1000 °C during isothermal ageing. However, the coarsening of the cuboidal precipitates and development of spontaneous rafts are not homogeneous within the microstructure. The coarsening rate is higher and formation of spontaneous rafts is faster within the dendrites than in the interdendritic region. Similar inhomogeneity in formation of the rafts is also observed during creep, as shown in Fig. 3. Nabarro et al. [15] showed that the driving force for development and orientation of the  $\gamma'$  rafts is: (i) the lattice misfit between  $\gamma'$  precipitates and the  $\gamma$  matrix, (ii) elastic mismatch between the  $\gamma'$  precipitates and the  $\gamma$  matrix and (iii) level of applied external stresses. The misfit parameter  $\delta$  defined as  $\delta = 2(a_{\gamma'} - a_{\gamma}) / (a_{\gamma'} + a_{\gamma})$ , where  $a_{\gamma}$  is lattice parameter of the  $\gamma$  matrix and  $a_{\gamma'}$  is the lattice parameter of the  $\gamma'$  precipitates. Brückner et al. [16] showed that this difference is negative of -0.29 % for primary dendrite arms, -0.19 % for secondary dendrite arms and positive of 0.03 % for the interdendritic region. Such differences in the misfit parameter and presence of internal stresses can explain inhomogeneous formation of the rafts in the studied superalloy during early stages of the creep.



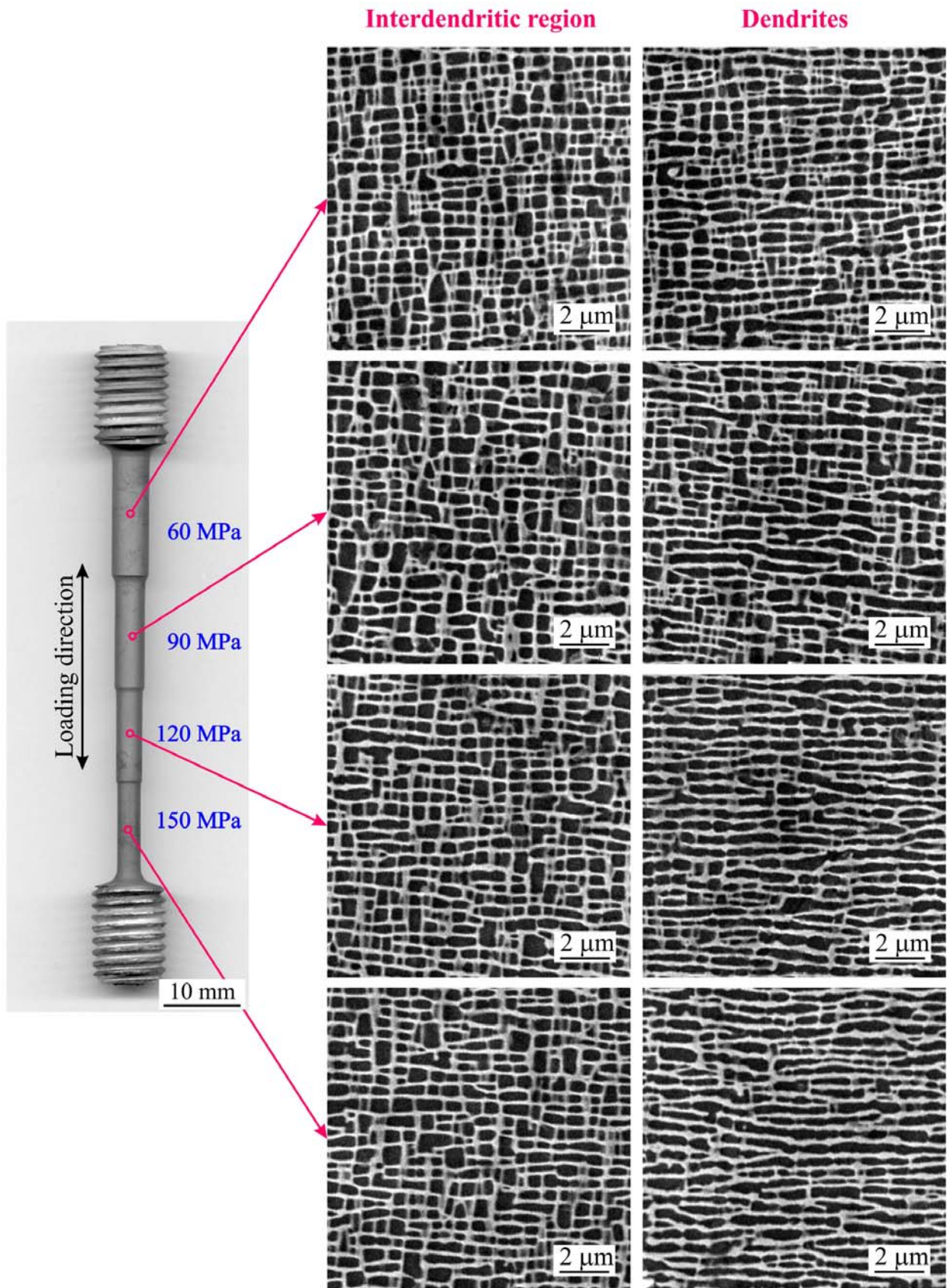


Fig. 3. Geometry of creep specimen with multiple gauge sections tested at a temperature of 950 °C for 500 h and evolution of the  $\gamma/\gamma'$  microstructure within the gauge sections subjected to applied stresses of 60, 90, 120 and 150 MPa.

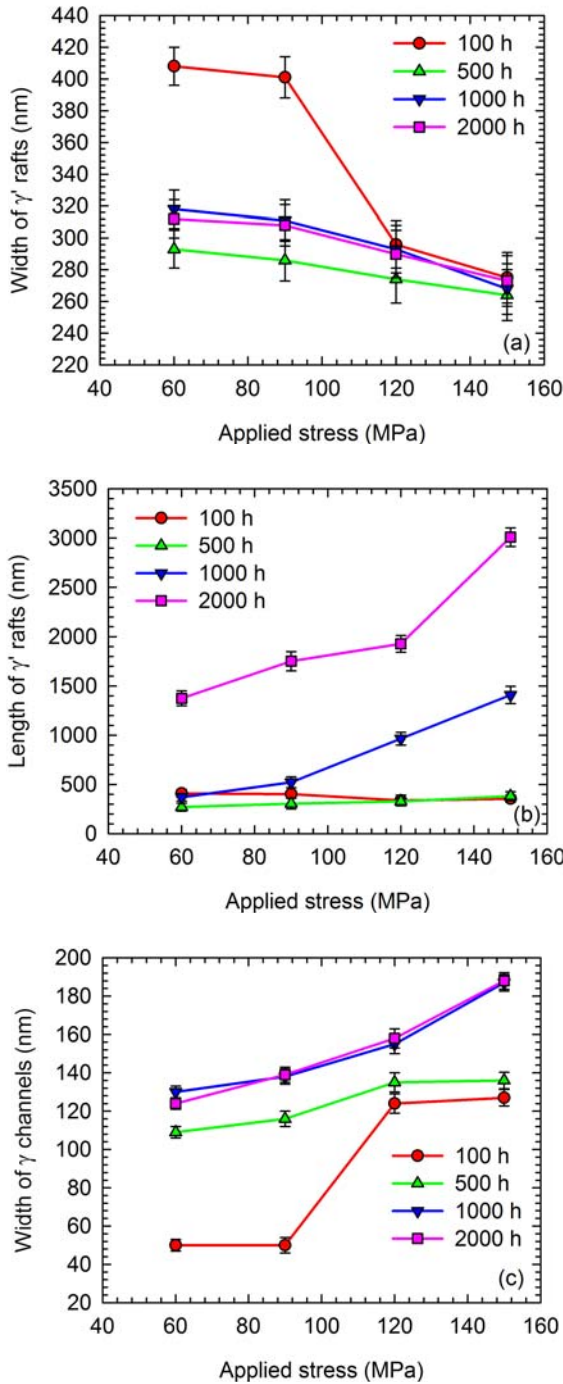


Fig. 4. Dependence of microstructural parameters on the applied stress: (a) width of the  $\gamma'$  rafts; (b) length of the  $\gamma'$  rafts; (c) width of the  $\gamma$  channels. The applied temperatures are indicated in the figures.

### 3.3. Effect of microstructure degradation on tensile properties

The tensile results of the heat treated and creep degraded specimens at the temperatures ranging from 20 to 950 °C are illustrated in Fig. 5. The 0.2 % offset

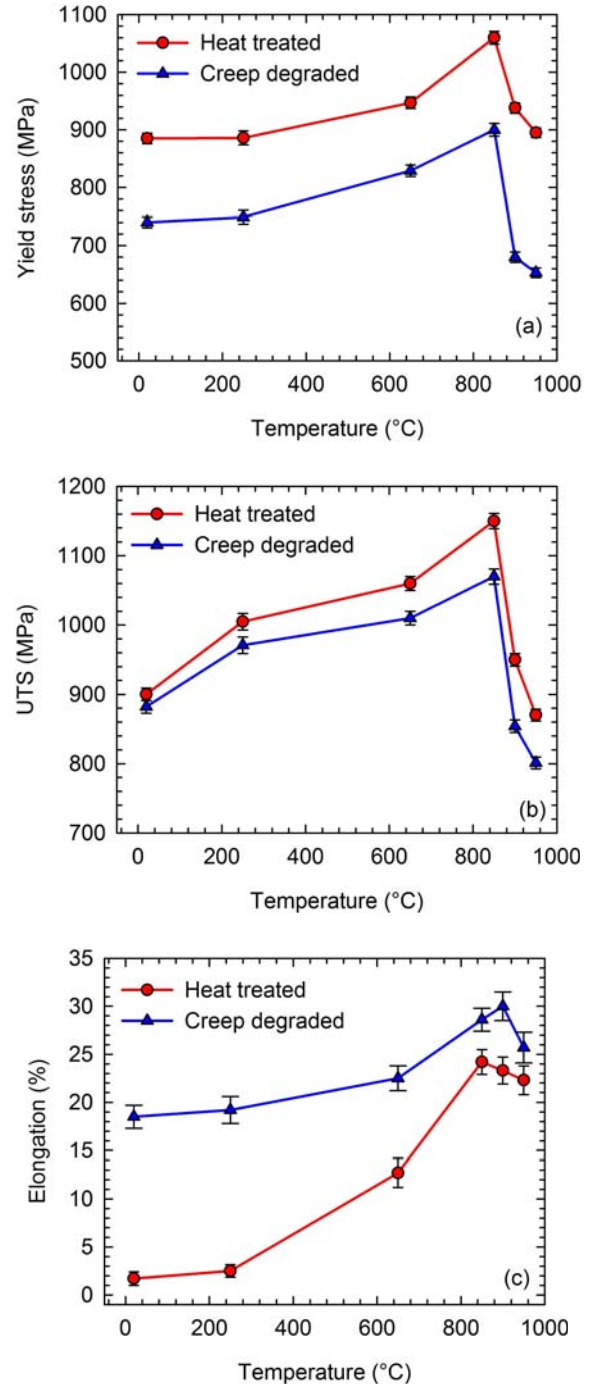


Fig. 5. Temperature dependence of tensile properties of heat treated and creep degraded specimens: (a) 0.2 % offset yield stress; (b) ultimate tensile strength, (c) plastic elongation to fracture.

yield stress and ultimate tensile strength (UTS) increase with increasing temperature up to about 800 °C and then both rapidly decrease with increasing temperature, as shown in Figs. 5a,b. As reported by Sengupta et al. [17], the peak values of the yield stress and UTS of the CMSX-4 superalloy strongly depend

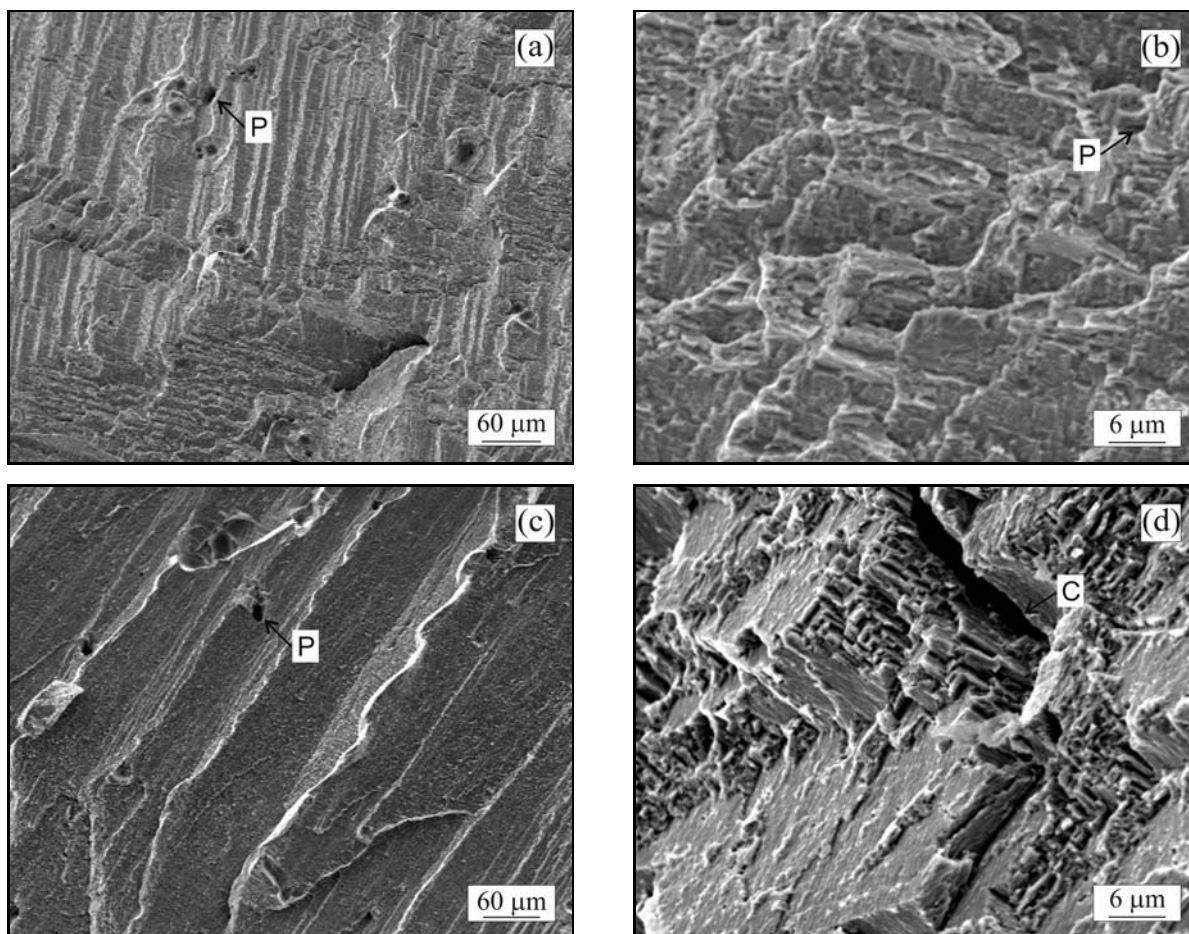


Fig. 6. SEM micrographs of fracture surface of tensile specimens tested at room temperature, P – porosity, C – crack: (a) and (b) heat treated specimens; (c) and (d) creep degraded specimens.

on particular microstructures resulting from the applied heat treatments but they achieve peak values at about 800 °C invariantly from the microstructure. The formation of the rafted microstructure during creep at 950 °C, applied stress of 230 MPa for 300 h decreases significantly yield stress and UTS but increases significantly the room and high temperature ductility, as shown in Fig. 5c. The decrease of the yield stress can be explained by strengthening mechanisms operating in the superalloy. For nickel based single crystal superalloys, the most important strengthening mechanism is the precipitation strengthening by the  $\gamma'$  particles. As shown by Lapin et al. [7], the size and volume fraction of the  $\gamma'$  particles significantly affect the yield strength of the CMSX-4 superalloy. The coarsening of the cuboidal precipitates decreases the yield stress and critical resolved shear stress (CRSS) [7]. The formation of the rafted microstructure leads to widening of the  $\gamma$  channels, which results in a further decrease of CRSS and yield stress when compared to coarsen one.

Figure 6 shows micrographs of fracture surface of the heat treated and creep degraded tensile specimens after tensile testing at room temperature. The palisade type of fracture surface in the heat treated

specimen is formed by propagation of cracks along (001) crystallographic planes in the directions parallel and perpendicular to the loading direction, as seen in Figs. 6a,b. The fracture surface contains numerous dimples around the pores formed during the directional solidification. The palisade type of fracture with numerous dimples around the pores can be seen also on the fracture surface of the creep degraded specimen shown in Figs. 6c,d. Figure 7 shows fracture features of the heat treated and creep degraded tensile specimens tested at high temperatures. The palisade type fracture for both types of specimens is preserved, as shown in Figs. 7a to 7d. Longitudinal section in the vicinity of the fracture surface contains numerous cracks oriented nearly perpendicularly to loading direction, as seen in Fig. 7e. Figure 7f indicates that the cracks frequently nucleate on the pores and propagate along the  $\gamma/\gamma'$  interfaces.

#### 4. Conclusions

The investigation of the effect of creep exposure on microstructure stability and tensile properties of single



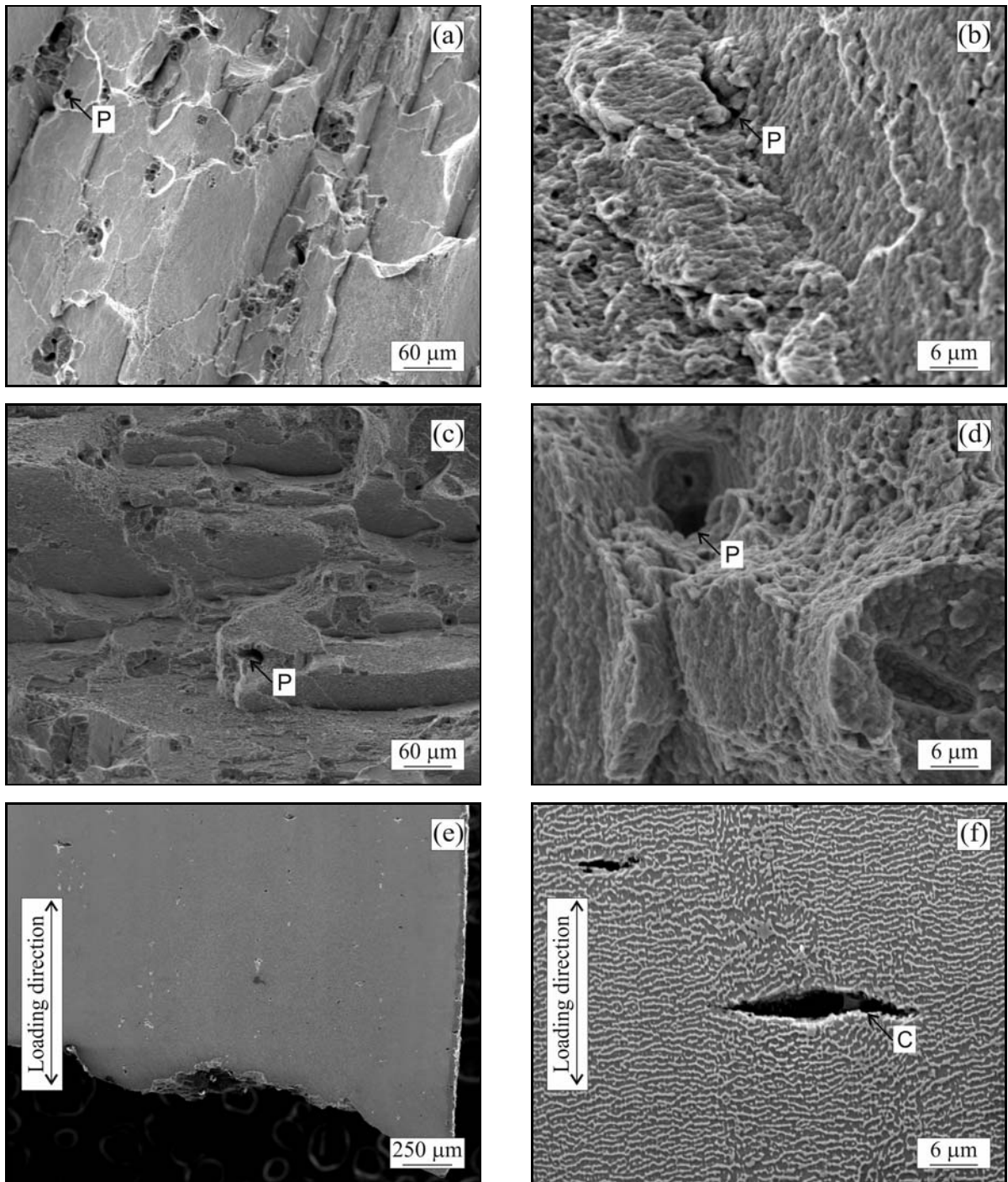


Fig. 7. SEM micrographs showing fracture features of tensile specimens tested at high temperatures, P – porosity, C – crack: (a) and (b) fracture surface of heat treated specimen tested at 850 °C; (c) and (d) fracture surface of creep degraded specimen tested at 850 °C; (e) and (f) longitudinal section in the vicinity of the fracture surface of creep degraded specimen tested at 900 °C.

crystal nickel based superalloy CMSX-4 suggests the following conclusions:

1. The initial cuboidal  $\gamma/\gamma'$  microstructure of the studied superalloy is unstable and undergoes three degradation stages during creep exposure at 950 °C: (i) coarsening of cuboidal  $\gamma'$  precipitates, (ii) formation of transient microstructure composed of coarsened and

rafted  $\gamma'$  precipitates and (iii) development of fully rafted  $\gamma/\gamma'$  microstructure.

2. The width of the  $\gamma'$  rafts decreases and their length increases with increasing applied stress and creep time. The width of the  $\gamma$  (Ni-based solid solution) channels increases with increasing applied stress and creep time.

3. The offset yield stress and UTS of the specimens with cuboidal and rafted  $\gamma/\gamma'$  microstructure increase with increasing temperature up to about 800 °C and then rapidly decrease at higher temperatures. The creep rafting decreases the yield stress and UTS when compared to those of the heat treated specimens with cuboidal  $\gamma/\gamma'$  microstructure in the temperature range from 20 to 950 °C. On the other hand, creep rafting increases significantly the room and high temperature ductility of the studied alloy.

4. The creep fracture surfaces exhibit palisade morphology formed by propagation of cracks along (001) planes in directions perpendicular and parallel to the loading direction.

### Acknowledgements

This work was financially supported by the Slovak Grant Agency for Science under the contract VEGA 2/0157/10. One of the authors (J. Lapin) would like to acknowledge the support of the RMTVC project under the contract No. CZ.1.05/2.1.00/01.0040. The authors would like to express their gratitude to Ing. Oto Bajana and Soňa Kružlíková for technical help.

### References

- [1] Matan, N., Cox, D. C., Rae, C. M. F., Reed, R. C.: *Acta Mater.*, 47, 1999, p. 2031. [doi:10.1016/S1359-6454\(99\)00093-2](https://doi.org/10.1016/S1359-6454(99)00093-2)
- [2] Lukáš, P., Obrtlík, K., Kunz, L., Čadek, J.: *Kovove Mater.*, 36, 1998, p. 205.
- [3] Lukáš, P., Čadek, J., Kunz, L., Šustek, V.: *Kovove Mater.*, 35, 1997, p. 120.
- [4] Lukáš, P., Čadek, J., Kunz, L., Svoboda, M., Klusák, J.: *Kovove Mater.*, 43, 2005, p. 5.
- [5] Lapin, J., Gebura, M., Pelachová, T., Nazmy, M.: *Kovove Mater.*, 46, 2008, p. 313.
- [6] Gebura, M., Lapin, J.: *Defect and Diffusion Forum*, 297–301, 2010, p. 826. [doi:10.4028/www.scientific.net/DDF.297-301.826](https://doi.org/10.4028/www.scientific.net/DDF.297-301.826)
- [7] Lapin, J., Gebura, M., Bajana, O., Pelachová, T., Nazmy, M.: *Kovove Mater.*, 47, 2009, p. 129.
- [8] Gebura, M., Lapin, J.: In: 17th International Conference on Metallurgy and Materials Metal 2008. Ed.: Tanger, s.r.o., Ostrava 2008, CD ROM.
- [9] Gebura, M.: *Microstructure evolution and degradation of nickel based single crystal superalloy during heat treatment and creep*. [PhD thesis]. Slovak Technical University, MTF-13561-27981, 2010.
- [10] Serin, K., Göbenli, G., Eggeler, G.: *Mater. Sci. Eng. A*, 387–389, 2004, p. 133. [doi:10.1016/j.msea.2004.01.114](https://doi.org/10.1016/j.msea.2004.01.114)
- [11] Kamaraj, M., Serin, K., Kolbe, M., Eggeler, G.: *Mater. Sci. Eng. A*, 319–321, 2001, p. 796. [doi:10.1016/S0921-5093\(01\)00950-9](https://doi.org/10.1016/S0921-5093(01)00950-9)
- [12] Nazmy, M., Denk, J., Baumann, R., Künzler, A.: *Scripta Mater.*, 48, 2003, p. 519. [doi:10.1016/S1359-6462\(02\)00506-7](https://doi.org/10.1016/S1359-6462(02)00506-7)
- [13] Nazmy, M., Künzler, A., Denk, J., Baumann, R.: *Scripta Mater.*, 47, 2002, p. 521. [doi:10.1016/S1359-6462\(02\)00194-X](https://doi.org/10.1016/S1359-6462(02)00194-X)
- [14] Lapin, J., Pelachová, T., Gebura, M.: In: 21st International Conference on Metallurgy and Materials Metal 2012. Ed.: Tanger, s.r.o., Brno 2012, p. 1287.
- [15] Nabarro, F. R. N.: *Metall. Mater. Trans. A*, 27A, 1996, p. 513.
- [16] Brückner, U., Epishin, A., Link, T., Dressel, K.: *Mater. Sci. Eng. A*, 247, 1998, p. 23. [doi:10.1016/S0921-5093\(97\)00856-3](https://doi.org/10.1016/S0921-5093(97)00856-3)
- [17] Sengupta, A., Putatunda, S. K., Bartosiewicz, L., Hangas, J., Nailos, P. J., Peputapeck, M., Alberts, F. E.: *J. Mater. Eng. Perform.*, 3, 1994, p. 73.